ACES Asian Chemical Editorial Society

DOI: 10.1002/asia.202000620

CHEMISTRY AN ASIAN JOURNAL Full Paper

Antiproliferative Activity of Functionalized Histidine-derived Au(I) *bis*-NHC Complexes for Bioconjugation

Christian H. G. Jakob,[a] Bruno Dominelli,[a] Eva M. Hahn,[a] Tobias O. Berghausen,[a] Teresa Pinheiro,[b] Fernanda Marques,[c] Robert M. Reich,[a] João D. G. Correia,[c] and Fritz E. Kühn*[a]

Abstract: A series of histidine derived Au(I) *bis*-NHC complexes bearing different ester, amide and carboxylic acid functionalities as well as wingtip substituents is synthesized and characterized. The stability in aqueous media, *in vitro* cytotoxicity in a set of cancer cell lines (MCF7, PC3 and A2780/A2780cisR) along with the cellular uptake are evaluated. Stability tests suggest hydrolysis of the ester within 8 h, which might lead to deactivation. Furthermore, the *bis*-NHC system shows a sufficient stability against cysteine and the thiol containing peptide GSH. The benzyl ester and amide show the highest activity comparable to the benchmark compound cisplatin, with the ester only displaying a slightly lower cytotoxicity than the amide. A cellular uptake study revealed that the benzyl ester and the amide could have different intracellular distribution profiles but both complexes induce perturbations of the cellular physiological processes. The simple modifiability and high stability of the complexes provides a promising system for upcoming post modifications to enable targeted cancer therapy.

Introduction

Cisplatin and derivatives are highly potent anticancer drugs administered for the treatment of various types of cancers (e.g., ovarian carcinoma of epithelial origin and small cell lung carcinoma).[1] Owing to the mechanism of action of platinum-based drugs, fast growing healthy cells are also damaged and no selectivity is attained,[2] which frequently leads to severe side effects. Furthermore, treatment with these drugs often results in the development of chemoresistance, which may lead to therapeutic failure.[3] Therefore, in the last years, a great deal of effort has been dedicated to the discovery and biological evaluation of novel transition metal complexes with improved cytotoxic properties as alternatives to cisplatin and derivatives.[4] Au(I) complexes emerged as promising candidates mainly due to their specific mechanism of action.[4–5] Owing to the thiophilicity of the gold atom/ion, the enzyme thioredoxin reductase is inhibited in the presence of some Au complexes, leading to oxidative stress and cell death.[6] The most prominent example is auranofin, which has been tested in a phase II clinical study against chronic lymphocytic leukemia (www.clinicaltrials.gov). One possibility to modulate the cytotoxic properties of potential metal drugs relies on the use of coordinating ligands with different properties. Phosphines, classical ligands in inorganic and organometallic chemistry, are often replaced by N-heterocyclic carbene (NHCs) ligands due to their higher ligand-metal binding strength to prevent ligand exchange phenomena.[5c,7] Moreover, as a result of organic cationic transporters overexpression on cancer cells, charged cationic Au(I) complexes, namely charged *bis*-NHC systems, display improved selectivity towards those cells.[8] Nevertheless, the selectivity strongly depends on the cell line considered.[6a,c,8] One of the current strategies followed in order to increase the selectivity of metal drugs is based on the conjugation of biomolecules to the metal complex with the aim of targeting selectively a disease related biomarker (e.g. transporter, enzyme or membrane receptor) overexpressed on cancer cells.[9] The type of biomolecules used are different in nature and may include hormones,[10] sugars[11] or peptides[12] conjugated to the complex *via* post modification.[13] Various Au(I) NHC-complexes bearing functional groups, including hydroxyl-,[14] carboxylic acid-,[15] nitrile-,[16] sulfonyl-[17] or amino acid functionalities,[18] amongst others, have been reported. However, only a few Au-NHCs bearing a suitable functional group for post modifications and conjugation to biomolecules are available. Moreover, examples of Au complexes attached to carrier targeting molecules are scarce.[19]

[a] C. H. G. Jakob, Dr. B. Dominelli, Dr. E. M. Hahn, T. O. Berghausen, Dr. R. M. Reich, Prof. Dr. F. E. Kühn
Molecular Catalysis
Catalysis Research Center and Department of Chemistry Department
Technische Universität München
Lichtenbergstrasse 4, D-85748 Garching bei München (Germany)
E-mail: fritz.kuehn@ch.tum.de

[b] Prof. Dr. T. Pinheiro
Institute for Bioengineering and Biosciences
Departamento de Engenharia e Ciências Nucleares
Instituto Superior Técnico
Universidade de Lisboa
Av. Rovisco Pais 1, 1049-001 Lisboa (Portugal)

[c] Dr. F. Marques, Prof. Dr. J. D. G. Correia
Centro de Ciências e Tecnologias Nucleares
Departamento de Engenharia e Ciências Nucleares
Instituto Superior Técnico
Universidade de Lisboa
CTN, Estrada Nacional 10 (km 139,7), 2695-066 Bobadela LRS (Portugal)

Supporting information for this article is available on the WWW under https://doi.org/10.1002/asia.202000620

One promising approach to post modifications is the use of amino acid derivatives as starting materials for ligand systems. Erker *et al.* proposed histidine as a NHC precursor and synthesized Pd complexes.[20] Further Ru,[21] Rh,[22] Pd[23] and Ir[24] complexes were reported for catalytic applications and only one Au(I) histidinylidene complex, with moderate IC_{50} values against various cancer cell lines, has been considered for medicinal applications.[18d] It is a neutral Au(I) complex bearing a Boc-protected α-amino-group, methyl wingtips and a methyl ester group, but neither the amino acid backbone was modified, nor the stability discussed.[18d]

Taking into account the observed correlation between the lipophilicity of metallodrugs – especially for Au complexes – and their antiproliferative activity, *bis*-NHCs with more lipophilic wingtips might present improved antiproliferative activity.[5a,25] Furthermore, deprotection of the amino acid functionality provides more simple post modification procedures *via* ester and amide formation in comparison to other reported post functionalization processes.[13,26] Based on those considerations, the synthesis and characterization of novel Au(I) histidinylidene complexes with different wingtips and modifications on the amino acid functionality in the backbone are reported in this work. Additionally, both stability and antiproliferative activity of these complexes towards various cancer lines is examined, as is the cellular uptake of selected candidate complexes. Based on the obtained results, the influence of the respective functional groups on the stability, antiproliferative activity and cellular uptake is discussed aiming to assess the potential application of the synthesized compounds as anticancer agents.

Results and Discussion

The overall synthetic procedures for the imidazolium salt precursors **1a** and **1b** as well for the Au(I) *bis*-NHC complexes **2a**, **2b**, **3a** and **3b** are displayed in scheme 1.

The imidazolium salts **1a** and **1b** were prepared in high yield by alkylation of N_α-Boc-*L*-histidine with methyl iodide or benzylbromide, respectively, as previously reported.[18d] They were characterized by elemental analysis, $^1H/^{13}C$-NMR spectroscopy and electrospray ionization mass spectrometry (ESI-MS). Both compounds are highly hygroscopic and soluble in polar solvents e.g. dichloromethane, acetonitrile and in water. The non-isolated intermediate Au(I) *bis*-NHC complexes **2a** and **2b** can be synthesized in a one-pot reaction by addition of Ag_2O and Au(THT)Cl, followed by exchange of the halogen anion with an acetate anion using silver acetate (scheme 1). The resulting crude complexes, which are soluble in common polar organic solvents but insoluble in water, have been treated with excess trifluoroacetic acid (TFA) to remove the Boc group, yielding the Au(I) *bis*-NHC complexes **3a** and **3b** (scheme 1). After reaction and adequate work-up, **3a** and **3b**, obtained as white solid, were lyophilized and obtained as TFA salts. These complexes, which display high stability towards TFA, were characterized by $^1H/^{13}C$-NMR spectroscopy, ESI-MS and elemental analysis. The most relevant features of the NMR spectra in both complexes is the absence of the imidazolium protons NC*H*N in the ^1H-NMR spectra and a significant downfield shift of the corresponding carbon signals to δ 186.1 in **3a** and to δ 185.0 ppm in **3b**. These shifts are in accordance with other previously reported Au(I) *bis*-carbene complexes.[27] Additionally the absence of the *t*-Bu groups, indicate a full deprotection. Furthermore, the integrals of the ester signals indicate a high stability towards hydrolysis under these conditions. The proton signals of the amino group are not detected due to a fast H/D exchange. The complexes **3a** and **3b** are soluble in various organic solvents, such as acetonitrile and dichloromethane, and exhibit moderate solubility in water. The straightforward synthetic strategy depicted in scheme 1 enables selective deprotection of one functional group in the backbone, allowing orthogonal post modification at the free *N*-terminus and further bioconjugation to carboxylic acid-containing biomolecules. However, the resulting complexes (**3a** and **3b**) still bear a pendant ester. This is, for biological applications, not the most adequate functional group considering the presence of esterases that might promote fast hydrolysis *in vivo*.[28]

Therefore, the ester functionality of compound **3b** is replaced by a more stable functional group, namely an amide group.[29]

To accomplish this goal two different strategies were investigated (scheme 2). Firstly, a post modification approach

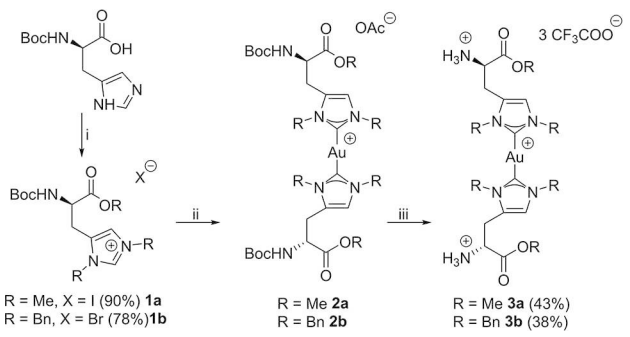

Scheme 1. Synthesis of imidazolium salts **1a** and **1b**; and of Au(I) *bis*-NHC complexes **2a**, **2b** (not isolated), **3a** and **3b**. i: $NaHCO_3$, RX, 110 °C, 16 h (MeCN); ii: 1. Ag_2O, Au(THT)Cl (THT = tetrahydrothiophene), r.t. 16 h (DCM); 2. AgOAc, 15 min, r.t., 3. TFA/DCM (5/1), r.t. 2 h.

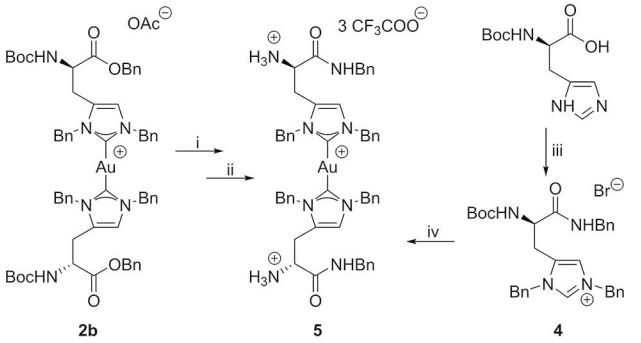

Scheme 2. Synthesis of the imidazolium salt 4 and complex 5 i: 1. LiOH, r.t. 1 h, (THF/H_2O) 2. 0.1 M TFA, r.t., 15 min; ii: TBTU, HOBt, r.t. 18 h (DMF). iii: 1. HOBt, EDC, r.t. 18 h, (DMF). 2. $NaHCO_3$, BnBr, 110 °C, 16 h (MeCN); iv 1. Ag_2O, Au(THT)Cl, r.t. 16 h (DCM); 2. AgOAc, 15 min, r.t. (MeCN) 3. TFA/DCM (5/1), r.t. 2 h.

was applied: the intermediate complex **2b** was treated with excess LiOH to quantitatively hydrolyze the intermediate ester complex. After *in situ* neutralization with 0.1 M TFA, the corresponding *bis*-benzylamide complex **5** was prepared under standard conditions as shown in scheme 2. A ca. 80% conversion was attained with the mono-amide complex being the main impurity, detected by analytical HPLC. However, separation of the *mono*-amide from the *bis*-amide is difficult and leads to low yields. Considering that laborious purification steps would be necessary to isolate complex **5** in significant yield, using the synthetic strategy described above, a second approach was applied. In the latter case, the *bis*-amide complex **5** was synthesized directly from N_α-Boc-*L*-histidine-benzylamide, followed by alkylation of the imidazole ring and final complex formation (scheme 2), similarly to the synthesis of **3a** and **3b**. As described for **3b** the absence of the *t*-Bu groups in ^{1}H- and ^{13}C-NMR clearly demonstrate the successful cleavage of the Boc-group.

To compare the influence of the backbone functional groups concerning cytotoxicity properties, complexes **6a** and **6b** with a pendant amino acid unit were prepared by treating the crude complexes **2a** and **2b** with LiOH for ester hydrolysis, followed by treatment with TFA for Boc deprotection (scheme 3). The complexes are stable against aqueous LiOH-solution under these conditions, which might be beneficial for further post modifications at the *C*-terminus. Both complexes **6a** and **6b** are insoluble in dichloromethane or acetonitrile, but highly soluble in water and dimethyl sulfoxide.

The complexes were characterized by ^{1}H/^{13}C-NMR spectroscopy, ESI-MS and elemental analysis. In the ^{1}H-NMR spectra, besides the absence of the corresponding ester and amide signals, no notable differences in comparison to the complexes **3** and **5** are observed. As mentioned before, the protons of the amino group and additionally of the carboxylic acid are not detected.

Stability in aqueous media

Since esters might undergo hydrolysis and, therefore, be unstable in aqueous biological environments the stability of **3a** and **3b** was further investigated. Hydrolysis leads to the formation of the corresponding more hydrophilic carboxylic compounds **6a** and **6b**. The stability was studied at 100 μM concentration, under the same conditions applied for testing the antiproliferative activity of the complexes described below. In brief, the metal complexes were incubated in RPMI culture medium at 37 °C for 48 h and samples were collected and analyzed by liquid chromatography (LC–MS) to identify and quantify possible decomposition products at different time points (0 h, 8 h, 24 h and 48 h).

Complex **3b** is completely hydrolyzed to the *mono*-ester and corresponding *di*-acid **6b** after 8 h incubation. Full conversion to **6b** is only observed after 48 h (see SI figures 22–25). Moreover, no additional decomposition peaks are detected in the HPLC chromatograms, indicating that the Au-NHC bond is stable during the whole incubation period. For complex **3a** a similar trend is observed, however, the hydrolysis kinetics is slower (see SI figures 18–21).

The stability of complex **3b** has been examined against *L*-cysteine and glutathione (GSH) as these thiol-containing molecules are present in blood proteins (*e.g.*, serum albumin), and may lead to decomposition or ligand exchange reactions by breaking the gold-NHC bond *via* nucleophilic attack of the SH-group.[5b,30] GSH is also the most abundant low molecular weight thiol compound in cells.[31]

By introducing a *bis*-NHC system a sufficient thiol stability might be achieved, compared to other ligands. In order to evaluate this assumption, the thiol stability was assessed by a time dependent ^{1}H-NMR spectroscopy study to get a deeper insight into possible decomposition pathways, *e.g.*, ligand exchange reactions (see SI figures 16 & 17). The thiol stability was only examined for one of those compounds, since they only differ in the functionalities in the backbone, which is not expected to affect the gold-NHC bond.

Interestingly, no decomposition could be observed in the presence of *L*-cysteine, even after 48 h incubation time at 37 °C (figure 1). In the case of incubation with GSH, only traces of a decomposition product are observed (δ 3.5 ppm, 4.6 ppm and 8.9 ppm) in the ^{1}H-NMR spectrum after 24 h, being assigned to the formation of an imidazolium salt *via* ligand protonation.

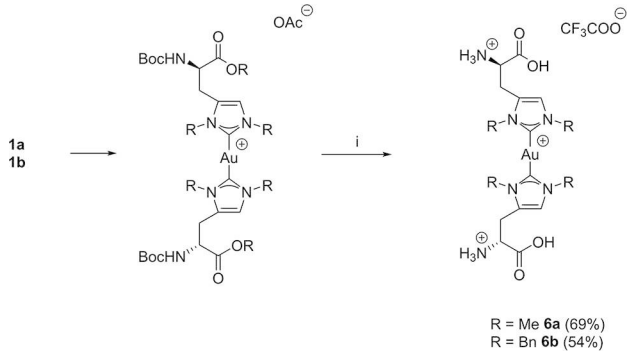

Scheme 3. Synthesis of complexes **6a** and **6b** i: 1. LiOH, r.t. 1 h, (THF/H_2O). 2. TFA/DCM (5/1), r.t. 2 h.

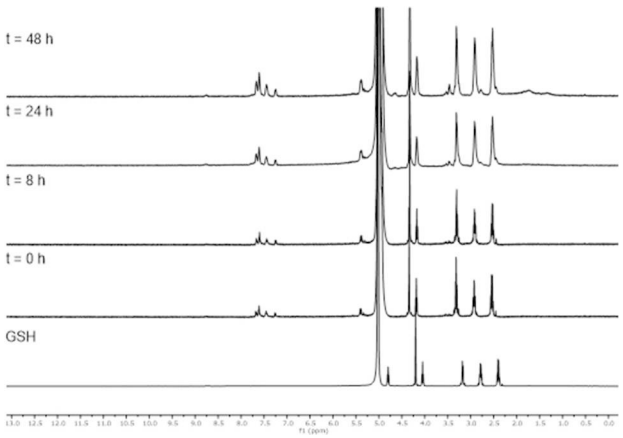

Figure 1. ^{1}H-NMR stability tests with **3b** and GSH in D_2O at 37 °C. The full spectra can be found in the SI figure 16.

These results demonstrate a remarkable stability of complex **3b** in the presence of *L*-cysteine and GSH.

The antiproliferative properties of complexes **3**, **5**, **6** and the reference metallodrugs cisplatin and auranofin were tested by monitoring their ability to inhibit the growth of selected cancer cell lines and a normal cell line (V79).

Their cytotoxic activity was determined on a set of cell lines representative of common human cancer diseases, PC3 (prostate), MCF7 (breast), A2780 and A2780cisR (ovarian, sensitive and resistant to cisplatin, respectively) and V79 a fibroblast cell line, by the MTT assay (table 1). Complexes **3a**, **6a** and **6b** display no activity against the above-mentioned cancer cell lines. This indicates that the introduction of methyl- and carboxylic acid groups leads to loss of activity. Due to the higher hydrophilicity, caused by the carboxylic acid functionalities, the cellular uptake may possibly be reduced.[15d,17a] However, complexes **3b** and **5** exhibit IC_{50} values comparable to a variety of other Au(I) complexes reported in literature, with an antiproliferative activity higher than that of cisplatin in MCF7 and A2780R.[5c,30b,32] Although complex **3b** hydrolyzes slowly to the non-active compound **6b** as discussed above, its cytotoxic activity is still substantial. This result suggests that hydrolysis of the compound might mainly occur after cell uptake and internalization. However, after hydrolysis of compound **3b** to **6** it could potentially not cross the cell membrane, leading to a deactivation. Complex **5** is more stable, which might lead to a higher activity, since no deactivation is observed over the whole incubation time. Especially for both A2780 cell lines a remarkable difference is observed.

The activity of **3b** and **5** is superior to the known Au(I) histidinylidene complex, corroborating the previously reported correlation between lipophilicity of the wingtips and antiproliferative activity.[7a,18d,25b,33] Furthermore, both complexes **3b** and **5** show a comparable activity in the cisplatin resistant cell line A2780cisR and in the respective cisplatin sensitive cell line. The complexes in general show a slightly higher cytotoxicity in cancer cells, compared to the non-cancerous cell line V79, which is an advantage, when compared to auranofin. Except for the PC3 cell in which a lower cytotoxicity is observed compared to V79. The latter displays very high cytotoxicity for all studied cell lines.

Table 1. IC_{50} values (μM) found for complexes **3a**, **3b**, **5**, **6a**, **6b** and the reference metallodrugs cisplatin and auranofin after 48 h incubation time.

	PC3	MCF7	A2780cisR	A2780	V79
3a	>100	>100	>100		
3b	39±16	4.6±1.9	15±4.4	10.0±2.5	19±5.6
5	25±3.5	2.9±1.0	3.4±0.92	4.0±1.4	17±6.7
6a	>100	>100	>100		
6b	>100	>100	>100		
Cisplatin	34±5.5	21±6.3	23±2.6	3.6±1.3	6.7±2.7
Auranofin	2.4±1.9	0.28±0.14	0.64±0.07	0.43±0.23	0.27±0.1

Cellular uptake

The cellular uptake was assessed in PC3 cells after incubation with complexes **3b** and **5** at equimolar concentration (50 μM) during 2 h applying two approaches, i) total concentration of Au in cellular pellets and ii) imaging and quantitating Au in whole cells. In both approaches Au concentrations were determined by proton induced X-ray emission (PIXE), that consists in collecting the characteristic X-rays emitted by the atoms of the sample, following their ionization by the incident protons. This enables quantification of all elements (for $Z > 11$) as X-ray yields are proportional to the mass of that element in the sample, with a sensitivity down to a few μg/g in concentration.[34]

The Au concentration in the cell pellets for complex **3b** was higher than for complex **5** (3700±2 μg/g vs 2000±13 μg/g dry weight), although **5** seems to be slightly more active than **3b** in this cell line (see Table 1). Figure 2 depicts the concentration of Au in the pellet normalized to the number of cells.

Correlating nuclear microscopy images of mass density with spatial distribution of the chemical elements selected from the PIXE spectra, it can be inferred that higher P contents associated with the high-density nuclear region and K and Ca were evenly distributed across cells (Figure 3 A). Au was virtually absent in cells treated with complex **3b** (Figure 3 A upper panel), while cells incubated with complex **5** showed a scattered distribution of Au (Figure 3 A lower panel), hindering the association of Au with cellular compartments. Quantitative analysis confirmed that Au was not detectable in cells with complex **3b** while in cells with complex **5**, Au was only determined in dispersed spots with concentrations varying from 200 μg/g to 2000 μg/g dry weigh. In terms of whole cell volume, the total Au content was of 795±275 μg/g dry weight. Therefore, the Au concentration in individual cells with complex **5** was comparable to the concentration in the pellet whereas in cells with **3b** complex the Au seems to be removed during the washing procedure together with the medium, suggesting that the complex may be loosely bound to the cells. These observations suggest that during the incubation period of 2 h,

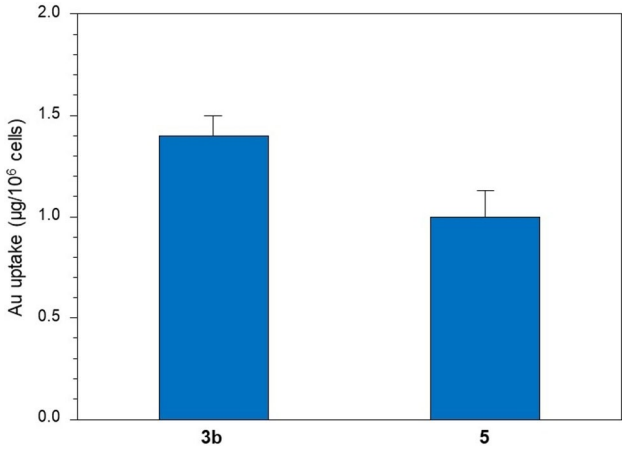

Figure 2. Au uptake in PC3 cells incubated with complexes **3b** and **5** (50 μM) for 2 h. Results are mean±SD of two experiments.

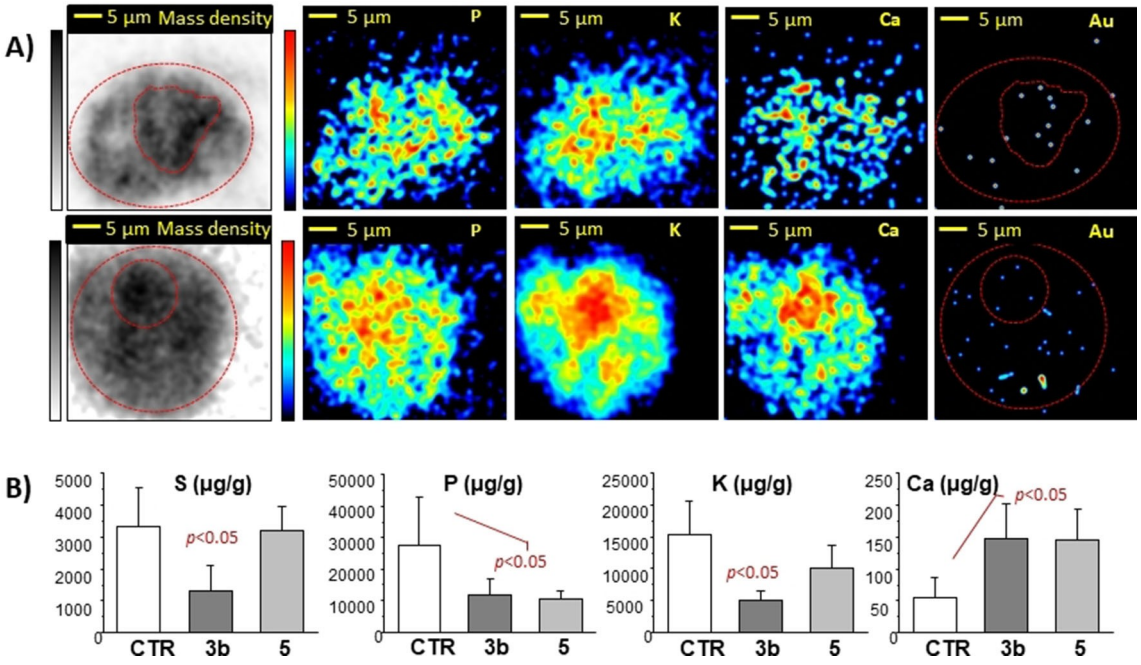

Figure 3. A) Mass density and elemental maps of spatial distribution of P, K, Ca and Au in individualized PC3 treated cells by nuclear microscopy: complexes **3b** (upper panel) and **5** complexes. The dotted lines in mass and Au maps indicate the cell contour and the nuclear region. The mass density and elemental distribution are represented by a colour gradient with a dynamic scale: high level- black/red; low level- white/deep blue. B) Concentrations of S, P, K and Ca (µg/g dry weight) in cells. Significant differences indicated ($p < 0.5$) relative to controls (non-treated cells).

3b complex was weakly retained at the cell surface whereas complex **5** was uptaken by PC3 cells. Nevertheless, **3b** can interact with vital components at the membrane causing important physiological changes.[35] The total concentrations of S, P, K and Ca assessed in whole cells, (controls and incubated with complexes **3b** and **5**) were more pronounced in cells incubated with **3b** complex than in those incubated with complex **5** (figure 3- B). For the cells treated with **3b** the S content significantly decreased relative to controls suggesting a loss of cellular constituents and protein content, as S is a component of thiol groups abundant in the protein structure.[36] Also, a significant decrease of P and K and an increase of Ca contents relative to controls were observed in **3b** treated cells. The P and Ca changes in cells with complex **5** showed a similar trend. These changes may reflect perturbations in regulatory pathways dependent on phosphorylative signaling[37] and cellular mechanisms regulating Ca^{2+} and K^{+} ions fluxes across membranes.[38]

Therefore, the results suggest that the interaction of complex **3b** with PC3 cells, possibly with cell surface domains and the uptake of complex **5** have both the ability to cause detrimental effects in these cells. This is in line with the similar activity of both complexes towards PC3 cells and with the verified lower stability of **3b** complex that may hamper its internalization.

Conclusion

A series of five novel Au(I) *bis*-histidinylidene complexes has been synthesized and characterized by ^{1}H- and ^{13}C-NMR, ESI-MS and elemental analysis. A variety of synthetic post modification routes of the amino-acid backbone is presented and discussed in order to examine an ideal basic structure for future bioconjugation. Additionally, the influence of the wingtip substituents and *C*-terminus modification on the antiproliferative activity in PC3, MCF7, A2780/A2780cisR and V79 cell lines was investigated suggesting that higher lipophilicity leads to a higher antiproliferative activity. The introduction of benzyl wingtips as well as ester and amide, respectively (complex **3b** and **5**), results in a high cytotoxicity, that is comparable to cisplatin and even active in the cisplatin resistant cell line A2780cisR. Although the ester slowly hydrolyzes as shown by stability tests, the complex only shows a slightly lower activity compared to the corresponding amide and cisplatin, which might result from fast uptake of the compound. The cellular uptake studies revealed that **3a** and **5** could have different distribution profiles. Morphological alterations and imbalance of elements essential for biologic processes suggest that **3b** effects are more severe, possibly by interacting with membranal vital systems. Nevertheless, both complexes induce perturbations of the cellular physiological processes. Despite the stability in the presence of cysteine and GSH, the selectivity against cancer cells is too low to justify further *in vivo* testing so far. However, this system provides an excellent opportunity to perform further post modifications with biomolecules (e.g. integrin-, PSMA-ligands or sugars) to increase the selectivity

due to its promising cytotoxicity, stability, easy accessibility and versatility. Further studies are under way in our laboratories to investigate the mechanism of action of these complexes in more detail.

Experimental Section

General procedures and analytical methods

All chemicals were purchased from commercial suppliers and used without further purification. All solvents were distilled prior to use. Unless noted otherwise, reactions were carried out under air. Au(THT)Cl,[39] **1a**,[18d] N_α-Boc-*L*-His-Benzylamide[40] were synthesized as reported. NMR Spectra were recorded on a Bruker AV 400 US, Bruker DRX-400 spectrometer or on a Bruker AV500C QNP Cryo probe at 300 K NMR. 2D NMR experiments were used for a correct assignment of the signals. Chemical shifts (δ) are reported relative to the residual signal of the deuterated solvent. Analytical reversed phase HPLC-HESI-MS (heated electrospray ionization mass spectrometry) was performed on an UltiMate 3000 UHPLC focused chromatographic system (Dionex) connected to a LCQ Fleet mass spectrometer (Thermo Scientific) equipped with a C18 column (ReproSil-XR 120 C18, 5 μm, 250×4.6 mm, Dr. Maisch). Linear gradients (1.0 mL/min, 30 min) of acetonitrile (0.1% formic acid) and water (0.1% formic acid) were used for analytical purpose. Semi-preparative reversed phase HPLC was performed on a Waters instrument: Waters 2545 (Binary Gradient Module), Waters SFO (System Fluidics Organizer), Waters 2996 (Photodiode Array Detector), Waters 2767 (Sample Manager) equipped with a C18-column (Reprosil-XR 120 C18, 5 μm, 250×25 mm, Dr. Maisch). Suitable linear gradients (40 mL/min) of H_2O (0.1% v/v trifluoroacetic acid (TFA)) and acetonitrile (0.1%v/v TFA) were applied for the purification of all compounds. Elemental analyses were carried out by the microanalytical laboratory at *Technische Universität München*. Cytotoxic activity was performed using a plate spectrophotometer (Power Wave Xs, Bio-Tek).

Synthesis procedures

Synthesis of imidazolium salt 1b

The synthesis is similar to that reported in the literature.[18d]

N_α-Boc-*L*-histidine (600 mg, 2.35 mmol, 1.00 eq) and $NaHCO_3$ (987 mg, 11.8 mmol, 5.00 eq) are suspended in MeCN (50 mL) and stirred for 1 h at room temperature. After addition of benzylbromide (2.01 g, 1.40 mL, 11.8 mmol, 5.00 eq) the suspension was stirred for 16 h at 110 °C. The suspension was cooled to room temperature and filtered over celite. After removal of the solvent *in vacuo*, the residue was dissolved in DCM, filtered over celite and the product was precipitated by addition of pentane and further washed with diethyl ether.

1b was obtained as a pale yellow solid in 78% yield (1.19 g, 1.83 mmol).

^{1}H NMR (400 MHz, CD_3CN) δ(ppm): 8.83 (s, 1H, NCHN), 7.40 (m, 15H, H_{Ph}), 6.10 (d, ^3J=8.6 Hz, 1H, NH), 5.35 (d, ^4J=3.6 Hz, 2H, NCH_2Ph), 5.29 (s, 2H, NCH_2Ph), 5.10 (s, 2H, OCH_2Ph), 4.35 (q, ^3J=7.5 Hz, 1H, CH_2CHNH) 3.07 (m, 2H, CH_2CHNH), 1.32 (s, 9H, $C(CH_3)_3$).

^{13}C NMR (101 MHz, CD_3CN) δ 171.2, (*C*OOBn), 156.4 ($NCOO^tBu$), 136.9 (NCHN), 136.4 (C_{Ph}) 134.70 (C_{Ph}), 133.98 (C_{Ph}), 133.12 (C_{Ph}), 130.21 (C_{Ph}), 130.13 (C_{Ph}), 130.07 (C_{Ph}), 129.98 (C_{Ph}), 129.48 (C_{Ph}), 129.27 (C_{Ph}), 129.09 (C_{Ph}), 121.82 (NCHC), 80.50 ($C(CH_3)_3$), 67.95 (OCH_2Ph), 53.73 (NCH_2Ph), 52.77 (CH_2CHNH), 51.55 (NCH_2Ph), 28.37 ($C(CH_3)_3$), 26.55 (CH_2CHNH).

ESI-MS (*m/z*) $[M-Br^-]^+$: calcd.: 526.27, found: 526.22

EA calcd.: C, 63.37; H, 5.98; N, 6.93. Found: C, 62.95; H, 6.00; N, 6.72.

Synthesis of complex 3a

Imidazolium salt **1a** (290 mg, 0.766 mmol, 2.00 eq) is dissolved in DCM (10 mL) and Ag_2O 88.8 mg (0.383 mmol, 1.00 eq) is added in solid. The suspension is stirred at room temperature for 30 min and Au(THT)Cl (123 mg,0.383 mmol, 1.00 eq) is added. The suspension is stirred at room temperature for further 16 h. Subsequently, the suspension is filtered over celite and the solvent is removed *in vacuo*. The crude product is dissolved in MeCN, silver acetate (70.4 mg, 0.422 mmol, 1.10 eq) is added and stirred for 15 min at room temperature. After filtration over celite the solvent is removed *in vacuo*. The crude product is dissolved in DCM (5 mL), treated with TFA (1.0 mL) and the reaction allowed to stir for two hours at room temperature. The solvent is removed *in vacuo* and the crude product is purified by semi preparative HPLC (MeCN/H_2O 5-95%, 15 min) t_r=5.8 min.

The product is obtained as colourless solid in 43% yield (152 mg, 0.163 mmol).

^{1}H NMR (400 MHz, CD_3CN) δ (ppm): 7.17 (s, 2H, NCHC), 4.30 (t, ^3J=7.0 Hz, 2H, $CHNH_2$), 3.80 (s, 6H, NCH_3), 3.80 (s, 6H, NCH_3), 3.79 (s, 6H, OCH_3), 3.35 (d, ^3J=7.0 Hz, 4H, CH_2CHNH_2).

^{13}C NMR (126 MHz, CD_3CN) δ(ppm): 186.1 (NCN), 169.6 (*C*OOMe), 128.9 (*N*CHC), 123.6 (NCH*C*), 53.9 (OCH_3), 52.3 (CH_2CHNH_2), 38.3 (NCH_3), 35.8 (NCH_3), 25.5 (CH_2CHNH_2).

ESI-MS (*m/z*) $[M-CF_3COO^-]^+$: calcd.: 591.20, found: 591.25

EA calcd.: C, 30.91; H, 3.46; N, 9.01. Found: C, 30.45; H, 3.45; N, 8.72.

Synthesis of complex 3b

The complex is synthesized as previously described for **3a**. 400 mg (0.590 mmol, 2.00 eq) **1b** is used as starting material. The crude product is purified by semi preparative HPLC (MeCN/H_2O 5–95%, 15 min) t_r=10.8 min

The product is obtained as colourless solid in 38% yield (157 mg, 0.130 mmol).

^{1}H NMR (500 MHz, CD_3CN) δ(ppm): 7.40–7.10 (m, 30H, H_{Ph}), 7.01 (d, ^4J=7.2 Hz, 2H, NCHC), 5.27–5.16 (m, 4H, NCH_2Ph), 5.13 (s, 4H, NCH_2Ph), 5.10–5.03 (m, 4H, OCH_2Ph), 4.02 (t, ^3J=7.2 Hz, 2H, CH_2CHNH_2), 3.17 (dd, ^2J=16.0, ^3J=7.2 Hz, 2H, CH_2CHNH_2), 3.09 (dd, ^2J=16.0, ^3J=7.2 Hz, 2H, CH_2CHNH_2).

^{13}C NMR (126 MHz, CD_3CN) δ(ppm): 185.0 (NCN), 168.3 (COOBn), 136.3 (NCHC), 135.8 (C_{Ph}), 134.9 (NCHC), 128.9 (C_{Ph}), 128.9 (C_{Ph}), 128.8 (C_{Ph}), 128.6 (C_{Ph}), 128.6 (C_{Ph}), 128.5 (C_{Ph}), 128.3 (C_{Ph}), 128.1 (C_{Ph}), 127.3 (C_{Ph}), 126.4 (C_{Ph}), 122.2 (C_{Ph}), 67.8 (OCH_2Ph), 54.3 (NCH_2Ph), 51.6 (NCH_2Ph), 51.5 (CH_2CHNH_2), 25.0 (CH_2CHNH_2).

ESI-MS (*m/z*) $[M-CF_3COO^-]^+$: calcd.: 1047.39 found: 1047.31

EA calcd. (+0.5 TFA): C, 50.67; H, 3.94; N, 5.81. Found: C, 50.69; H, 3.93; N, 5.80.

Synthesis of imidazolium salt 4

The imidazolium salt **4** is synthesized analogous to the synthesis of imidazolium salt **2b**. 2.01 g (5.87 mmol, 1.0 eq) Boc-His-NHBn is used as starting material.

The product is obtained as colourless solid in 79% (2.82 g, 4.66 mmol)

^{1}H NMR (400 MHz, CD_3CN) δ(ppm): 8.51 (s, 1H, NCHN), 7.51–7.17 (m, 17H, H_{Ph}, NH, NCHC), 5.84 (d, ^3J = 7.9 Hz, 1H, NH), 5.31 (s, 2H, NCH_2Ph), 5.25 (s, 2H, NCH_2Ph), 4.27 (m, 3H, CH_2CHNH, $NHCH_2Ph$), 3.09 (dd, ^2J = 15.9, ^3J = 5.3 Hz, 1H, CH_2CHNH), 2.89 (dd, ^2J = 15.9, ^3J = 8.7 Hz, 1H, CH_2CHNH), 1.35 (s, 9H, $C(CH_3)_3$).

^{13}C NMR (101 MHz, CD_3CN) δ (ppm): 170.8 (CONHBn), 156.3 ($NCOO^tBu$), 139.74 (NCHN), 136.6 (C_{Ph}), 134.6 (C_{Ph}), 133.9 (C_{Ph}), 133.3 (C_{Ph}), 130.2 (C_{Ph}), 130.1 (C_{Ph}), 130.0 (C_{Ph}), 129.9 (C_{Ph}), 129.4 (C_{Ph}), 129.3 (C_{Ph}), 129.1 (C_{Ph}), 128.2 (C_{Ph}), 127.9 (C_{Ph}), 121.7 (NCHC), 80.5 ($C(CH_3)_3$), 53.7 (NCH_2Ph), 53.5 (NCH_2Ph), 51.4 (CH_2CHNH), 43.5 (CH_2CHNH), 28.3 ($C(CH_3)_3$), 27.0 (CH_2CHNH).

ESI-MS (*m/z*) $[M-Br^-]^+$: calcd.: 525.29, found: 525.22

EA calcd. ($C_{32}H_{37}BrN_4O_3$ + 0.5 H_2O): C, 62.54; H, 6.23; N, 9.12. Found: C, 62.71; H, 6.14; N, 9.23.

Synthesis of complex 5

The complex is synthesized as described for **3b**. 200 mg (0.333 mmol, 2.00 eq) the corresponding imidazolium **4** salt is used as starting material.

The crude product is purified by semi preparative HPLC (MeCN/H_2O 30–70%, 15 min) t_r = 9.98 min

The product is obtained as colourless solid in 26% yield (59.4 mg, 0.0430 mmol).

^{1}H NMR (400 MHz, CD_3CN) δ(ppm): 7.66 (t, ^3J = 6.3 Hz, 2H, NH), 7.32–7.24 (m, 18H, H_{Ph}), 7.17–7.11 (m, 10H, H_{Ph}), 7.07–6.97 (m, 4H, H_{Ph}, NCHC), 5.23 (s, 4H, NCH_2Ph), 5.14 (s, 4H, NCH_2Ph), 4.26–4.21 (m, 4H, $NHCH_2Ph$), 3.98 (t, ^3J = 6.7 Hz, 2H, CH_2CHNH_2), 3.01 (d, ^3J = 6.7 Hz, 4H, CH_2CHNH_2).

^{13}C NMR (126 MHz, CD3CN) δ(ppm): 185.9 (NCN), 168.3 (CNHBn), 139.0 (NCHC), 137.14 (NCHC), 136.87 (C_{Ph}), 129.83 (C_{Ph}), 129.78 (C_{Ph}), 129.42 (C_{Ph}), 129.18 (C_{Ph}), 129.00 (C_{Ph}), 128.42 (C_{Ph}), 128.21 (C_{Ph}), 127.24 (C_{Ph}), 123.03 (C_{Ph}), 55.23 ($CONHCH_2Ph$), 52.90 ($NHCH_2Ph$), 52.30 ($NHCH_2Ph$), 26.79 (CH_2CHNH_2).

ESI-MS (*m/z*) $[M-CF_3COO^-]^+$: calcd.: 1045.42, found: 1045.44

EA calcd.: C, 51.95; H, 4.21; N, 8.08. Found: C, 51.29; H, 4.36; N, 7.99.

EA calcd.(+1 H_2O): C, 51.29; H, 4.30; N, 7.97. Found: C, 51.29; H, 4.36; N, 7.99.

Synthesis of 6a

300 mg (0.705 mmol, 2.00 eq) imidazoliumsalt **1a** is dissolved in 10 mL DCM. 81.7 mg (0.353 mmol, 1.00 eq) Ag_2O is added and the suspension is stirred at room temperature for one hour. After the addition of 124 mg (0.388 mmol, 1.10 eq) Au(THT)Cl the suspension is stirred at room temperature for further 16 h. Subsequently, the suspension is filtered over celite and the solvent is removed *in vacuo*. The crude product is dissolved in MeCN and 64.8 mg (0.388 mmol, 1.10 eq) silver acetate is added and stirred for 15 min at room temperature. After filtration over celite the solvent is removed *in vacuo*. The crude product is dissolved in a mixture of 10 mL THF and 5 mL H_2O and 84.6 mg (3.53 mmol, 10.0 eq) LiOH is added and the solution is stirred for one hour at room temperature. After filtration, the solvent is removed *in vacuo* dissolved in 5 mL DCM and treated with 1 mL TFA. After stirring for 2 h, the solvent is removed and the crude product is purified by semi preparative HPLC (MeCN/H_2O 5–95%, 15 min) t_r = 5.3 min

The product is obtained as colourless solid in 69% (219 mg, 0.242 mmol).

^{1}H NMR (400 MHz, DMSO) δ(ppm): 7.30 (s, 2H, NCHC), 4.06 (t, ^3J = 6.8 Hz, 2H, $CHNH_2$), 3.80 (s, 6H, NCH_3), 3.23 (dd, ^2J = 15.9, ^3J = 5.7 Hz, 4H, CH_2CHNH_2), 3.10 (dd, ^2J = 16.0, 7.7 Hz, 4H, CH_2CHNH_2).

^{13}C NMR (101 MHz, DMSO) δ 183.67 (NCN), 169.70 (COOH), 128.75 (NCHC), 122.60 (NCHC), 51.30 (CH_2CHNH_2), 37.51 (NCH_3), 35.09 (NCH_3), 24.91 (CH_2CHNH_2).

ESI-MS (*m/z*) $[M-CF_3COO^-]^+$: calcd.: 563.17, found: 563.18

EA calcd.: C, 29.22; H, 3.12; N, 9.29. Found: C, 29.14; H, 3.48; N, 9.74.

Synthesis of complex 6b

The complex was synthesized as described for **6a**. 201 mg (0.151 mmol, 2.00 eq) of Imidazolium salt **1b** is used as starting material.

The crude product is purified by semi preparative HPLC (MeCN/H2O 5–95%, 15 min) t_r = 8.67 min

The product is obtained as colourless solid in 54% yield (99.0 mg, 0.0820 mmol).

^{1}H NMR (400 MHz, DMSO) δ(ppm): 7.51 (s, 2H, NCHC), 7.38–7.23 (m, 12H, H_{Ph}), 7.22–7.16 (m, 4H, H_{Ph}), 7.15–7.04 (m, 4H, H_{Ph}), 5.34 (s, 2H, NCH_2Ph), 5.29 (s, 2H, NCH_2Ph), 4.00 (t, ^3J = 6.4 Hz, 2H, $CHNH_2$), 3.02 (dd, ^2J = 16.1, ^3J = 6.4 Hz, 2H, CH_2CHNH_2), 2.93 (dd, ^2J = 16.1, ^3J = 6.4 Hz, 2H, CH_2CHNH_2).

^{13}C NMR (126 MHz, CD_3CN) δ(ppm): 183.4 (NCN), 168.6 (COOH), 136.7 (NCHC), 136.1 (C_{Ph}), 130.9 (NCHC), 128.8 (C_{Ph}), 128.6 (C_{Ph}), 128.0 (C_{Ph}), 127.9 (C_{Ph}), 127.3 (C_{Ph}), 126.4 (C_{Ph}), 121.6 (C_{Ph}), 53.7 (NCH_2Ph), 52.4 (NCH_2Ph), 50.9 (CH_2CHNH_2), 25.7 (CH_2CHNH_2).

ESI-MS (*m/z*) $[M-CF_3COO^-]^+$: calcd.: 867.29 found: 867.33

EA calcd.: C, 45.71; H, 3.67; N, 6.95. Found: C, 45.73; H, 3.63; N, 6.87.

Stability tests in aqueous media

100 μL of a 10 mM stock solution of the complexes in DMSO is prepared and diluted with RPMI medium to a final concentration of 0.1 mM. The solution was stirred at 37 °C for 48 h and analysed by HPLC-MS (5 μL injection volume, 30 min). Measurements were conducted at different time periods.

Thiol stability: **3b** was dissolved (2.5 mg in 0.5 mL D_2O) and 5.0 eq Cysteine or GSH are added in solid. The sample was incubated at 37 °C and ^{1}H-NMR measurements were conducted at different times

Cytotoxic activity

The cytotoxic activity of the test compounds is evaluated in several human cancer cells, PC3 (ATCC), MCF7 (ATCC), A2780 and A2780cisR (Sigma-Aldrich) and a non-tumoral cell line V79 (ATCC). All cell lines are grown in RPMI medium supplemented with 10% FBS and maintained at 37 °C in an incubator (Heraeus, Germany) with 5% CO_2 and humidified atmosphere. The cellular viability is measured by the colorimetric MTT (3-(4,5-dimethythiazol2-yl)-2,5-diphenyl tetrazolium bromide) assay which is based on the

conversion of the tetrazolium salt to an insoluble formazan product by mitochondrial dehydrogenase enzymes active in living cells. For the assay, cells are seeded in 96-well plates at a density of $2x10^4$ cells/200 μL medium and allowed to adhere for 24 h. Complexes are first diluted in DMSO for complete solubility and then in medium to prepare serial dilutions in the range of 0.1 μM–100 μM. The maximum concentration of DMSO in the medium is 1% and at this percentage is without cytotoxic effect. The reference compounds cisplatin and auranofin are first diluted in water (cisplatin) and DMSO (auranofin) and then in medium in the same concentration range of the complexes. After careful removal of the medium, 200 μL of each compound's dilution in fresh medium are added to the cells and incubated for 48 h at 37 °C. At the end of the treatment, the medium is discarded and 200 μL of MTT solution in PBS (0.5 mg/ml) are applied to each well. After 3 h at 37 °C, the medium is removed and replaced by DMSO (200 μL) to solubilize the formazan crystals formed. The percentage of cellular viability is assessed measuring the absorbance at 570 nm. Dose-response curves are obtained after 48 h incubation using the GraphPad Prism software (version 5.0) and the corresponding IC_{50} values are calculated. Results are shown as the mean ± SD of at least two independent experiments done with six replicates per condition.

Cellular uptake

Elemental concentrations were assessed by proton induced X-ray emission (PIXE) technique in cellular pellets and individualized whole cells. This was achieved by using broad and focused proton beams of 2 MeV, respectively, generated at the Van de Graaff accelerator facility of Instituto Superior Técnico (IST).[41a;b]

Total concentration of Au in cellular pellets

PC3 cells (~10^6 cells/5 mL medium) were seeded in T25 culture flasks and allowed to adhere for 24 h. Then the medium was replaced with 5 mL of each complex **3b** or **5** in medium at 50 μM in medium and the cells were incubated for 2 h. After the incubation period cells were washed with PBS and centrifuged to obtain a cellular pellet. The pellets were acid digested in a 1:3 molar ratio mixture of nitric and hydrochloric acids together with Y as an internal standard, combining ultrasound cycles of 30 min at 60 °C and microwave-assisted acid digestion (350 W, 15 s), as described in literature.[42] Aliquots of the resulting solution were analyzed by PIXE. Concentrations were expressed in μg/g of dry material and normalized to μg/10^6 cells.

Imaging and quantifying elemental localization in whole cells

PC3 cells were seeded on 100 nm thick silicon nitride membranes (Silson Ltd., UK), and incubated with complexes 3b and 5 under the same conditions as referred above *i.e.*, incubation for 2 h at 50 μM. The monolayer of cells on the silicon nitride membranes was washed with cold PBS and freeze-dried before being analyzed in vacuum by nuclear microscopy to image and quantify elemental distributions in cells.[b38] A focused proton beam with micrometer spatial resolution can provide images of the mass density of cryopreserved cells in transmission mode (i.e., remaining energy of the protons after going through the sample is measured, at each position of the beam using scanning transmission ion microscopy technique), and simultaneously enable the visualization of elemental concentrations by detecting the characteristic X-rays emitted by the elements (PIXE technique) at each position of the beam. Images are produced in real-time and the acquired elemental data can be processed to yield fully quantitative results for regions of interest selected from maps. In its principle, quantification relies on cell matrix composition estimation to mass normalize the PIXE X-ray yields (i.e., analyzing the energy of the backscattered protons after suffering elastic collisions with the nuclei of atoms in the sample at each position of the beam using Rutherford backscattering spectrometry technique).[41a] Acquisition of data and analysis was performed using OMDAQ 2007 (Oxford Microbeams Ltd, UK).[43]

Acknowledgements

C.H.G. Jakob and B. Dominelli acknowledge the TUM graduate for financial support. J. D. G. Correia acknowledges the support of the Fundação para a Ciência e Tecnologia (FCT), Portugal, through the projects UID/Multi/04349/2019 and PTDC/QUI-NUC/30147/2017. C. H. G. Jakob thanks S. Deiser for experimental support. T. Pinheiro acknowledges the support of the FCT through the projects UID/BIO/04565/2020 and Programa Operacional Regional de Lisboa 2020 (Project N. 007317). Open access funding enabled and organized by Projekt DEAL.

Conflict of Interest

The authors declare no conflict of interest.

Keywords: N-Heterocyclic Carbenes · Gold · Medicinal Chemistry · Anti-cancer · Amino acid

[1] a) B. Rosenberg, L. Van Camp, T. Krigas, *Nature* **1965**, *205*, 698–699; b) B. Rosenberg, L. Vancamp, J. E. Trosko, V. H. Mansour, *Nature* **1969**, *222*, 385–386; c) M. G. Apps, E. H. Y. Choi, N. J. Wheate, *Endocr.-Relat. Cancer* **2015**, *22*, R219.
[2] S. Dasari, P. Bernard Tchounwou, *Eur. J. Pharmacol.* **2014**, *740*, 364–378.
[3] a) A.-M. Florea, D. Büsselberg, *Cancers* **2011**, *3*, 1351–1371; b) M. Komatsu, T. Sumizawa, M. Mutoh, Z.-S. Chen, K. Terada, T. Furukawa, X.-L. Yang, H. Gao, N. Miura, T. Sugiyama, S.-i. Akiyama, *Cancer Res.* **2000**, *60*, 1312–1316.
[4] W. Liu, R. Gust, *Coord. Chem. Rev.* **2016**, *329*, 191–213.
[5] a) M. V. Baker, P. J. Barnard, S. J. Berners-Price, S. K. Brayshaw, J. L. Hickey, B. W. Skelton, A. H. White, *Dalton Trans.* **2006**, 3708–3715; b) C. F. Shaw, *Chem. Rev.* **1999**, *99*, 2589–2600; c) M. Mora, M. C. Gimeno, R. Visbal, *Chem. Soc. Rev.* **2019**, *48*, 447–462.
[6] a) J. L. Hickey, R. A. Ruhayel, P. J. Barnard, M. V. Baker, S. J. Berners-Price, A. Filipovska, *J. Am. Chem. Soc.* **2008**, *130*, 12570–12571; b) P. J. Barnard, S. J. Berners-Price, *Coord. Chem. Rev.* **2007**, *251*, 1889–1902; c) A. Bindoli, M. P. Rigobello, G. Scutari, C. Gabbiani, A. Casini, L. Messori, *Coord. Chem. Rev.* **2009**, *253*, 1692–1707.
[7] a) B. Dominelli, J. D. G. Correia, F. E. Kühn, *J. Organomet. Chem.* **2018**, *866*, 153–164; b) W. A. Herrmann, C. Köcher, *Angew. Chem. Int. Ed.* **1997**, *36*, 2162–2187; *Angew. Chem.* **1997**, *109*, 2256–2282; c) T. Zou, C.-N. Lok, P.-K. Wan, Z.-F. Zhang, S.-K. Fung, C.-M. Che, *Curr. Opin. Chem. Biol.* **2018**, *43*, 30–36.
[8] S. B. Aher, P. N. Muskawar, K. Thenmozhi, P. R. Bhagat, *Eur. J. Med. Chem.* **2014**, *81*, 408–419.
[9] R. H. Fish, *J. Organomet. Chem.* **2015**, *782*, 3–16.
[10] E. Kim, P. T. Rye, J. M. Essigmann, R. G. Croy, *J. Inorg. Biochem.* **2009**, *103*, 256–261.
[11] R. Wai-Yin Sun, D.-L. Ma, E. L.-M. Wong, C.-M. Che, *Dalton Trans.* **2007**, 4884–4892.
[12] a) J. Han, A. F. B. Räder, F. Reichart, B. Aikman, M. N. Wenzel, B. Woods, M. Weinmüller, B. S. Ludwig, S. Stürup, G. M. M. Groothuis, H. P. Permentier, R. Bischoff, H. Kessler, P. Horvatovich, A. Casini, *Bioconjugate Chem.* **2018**, *29*, 3856–3865; b) A. O. Frank, E. Otto, C. Mas-Moruno, H. B. Schiller, L. Marinelli, S. Cosconati, A. Bochen, D. Vossmeyer, G. Zahn, R.

Stragies, E. Novellino, H. Kessler, *Angew. Chem. Int. Ed.* **2010**, *49*, 9278–9281; *Angew. Chem.* **2010**, *122*, 9465–9468; c) Y. Shen, M. Schottelius, K. Zelenka, M. De Simone, K. Pohle, H. Kessler, H.-J. Wester, P. Schmutz, R. Alberto, *Bioconjugate Chem.* **2013**, *24*, 26–35.
[13] B. Albada, N. Metzler-Nolte, *Chem. Rev.* **2016**, *116*, 11797–11839.
[14] a) J. Rieb, B. Dominelli, D. Mayer, C. Jandl, J. Drechsel, W. Heydenreuter, S. A. Sieber, F. E. Kühn, *Dalton Trans.* **2017**, *46*, 2722–2735; b) R. Zhong, A. Pöthig, D. C. Mayer, C. Jandl, P. J. Altmann, W. A. Herrmann, F. E. Kühn, *Organometallics* **2015**, *34*, 2573–2579; c) A. C. Lindhorst, M. Kaspar, P. J. Altmann, A. Pöthig, F. E. Kühn, *Dalton Trans.* **2018**, *47*, 1857–1867; d) T. Diehl, M. T. S. Krause, S. Ueberlein, S. Becker, A. Trommer, G. Schnakenburg, M. Engeser, *Dalton Trans.* **2017**, *46*, 2988–2997; e) C. Hemmert, R. Poteau, M. Laurent, H. Gornitzka, *J. Organomet. Chem.* **2013**, *745–746*, 242–250; f) B. Jacques, D. Hueber, S. Hameury, P. Braunstein, P. Pale, A. Blanc, P. de Frémont, *Organometallics* **2014**, *33*, 2326–2335.
[15] a) R. Puerta-Oteo, M. V. Jiménez, F. J. Lahoz, F. J. Modrego, V. Passarelli, J. J. Pérez-Torrente, *Inorganics* **2018**, *57*, 5526–5543; b) M. Pellei, V. Gandin, M. Marinelli, C. Marzano, M. Yousufuddin, H. V. R. Dias, C. Santini, *Inorganics* **2012**, *51*, 9873–9882; c) J. Cure, R. Poteau, I. C. Gerber, H. Gornitzka, C. Hemmert, *Organometallics* **2012**, *31*, 619–626; d) B. Dominelli, G. M. Roberts, C. Jandl, P. J. Fischer, R. M. Reich, A. Pöthig, J. D. G. Correia, F. E. Kühn, *Dalton Trans.* **2019**, ***48***, 14036–14043.
[16] S. Y. Hussaini, R. A. Haque, J.-H. Li, S.-Z. Zhan, K. W. Tan, M. R. Razali, *Appl. Organomet. Chem.* **2019**, *33*, e4927.
[17] a) Ö. Karaca, V. Scalcon, S. M. Meier-Menches, R. Bonsignore, J. M. J. L. Brouwer, F. Tonolo, A. Folda, M. P. Rigobello, F. E. Kühn, A. Casini, *Inorganics* **2017**, *56*, 14237–14250; b) E. A. Baquero, J. C. Flores, J. Perles, P. Gómez-Sal, E. de Jesús, *Organometallics* **2014**, *33*, 5470–5482.
[18] a) G. Xu, S. R. Gilbertson, *Org. Lett.* **2005**, *7*, 4605–4608; b) J. Lemke, A. Pinto, P. Niehoff, V. Vasylyeva, N. Metzler-Nolte, *Dalton Trans.* **2009**, 7063–7070; c) A. Gutiérrez, M. C. Gimeno, I. Marzo, N. Metzler-Nolte, *Eur. J. Inorg. Chem.* **2014**, *2014*, 2512–2519; d) F. Schmitt, K. Donnelly, J. K. Muenzner, T. Rehm, V. Novohradsky, V. Brabec, J. Kasparkova, M. Albrecht, R. Schobert, T. Mueller, *J. Inorg. Biochem.* **2016**, *163*, 221–228.
[19] a) M. V. Baker, P. J. Barnard, S. J. Berners-Price, S. K. Brayshaw, J. L. Hickey, B. W. Skelton, A. H. White, *J. of Organomet. Chem.* **2005**, *690*, 5625–5635; b) P. de Frémont, E. D. Stevens, M. D. Eelman, D. E. Fogg, S. P. Nolan, *Organometallics* **2006**, *25*, 5824–5828; c) W. Niu, X. Chen, W. Tan, A. S. Veige, *Angew. Chem. Int. Ed.* **2016**, *55*, 8889–8893; *Angew. Chem.* **2016**, *128*, 9035–9039.
[20] F. Hannig, G. Kehr, R. Fröhlich, G. Erker, *J. Organomet. Chem.* **2005**, *690*, 5959–5972.
[21] A. Monney, G. Venkatachalam, M. Albrecht, *Dalton Trans.* **2011**, *40*, 2716–2719.
[22] a) A. Monney, M. Albrecht, *Chem. Commun.* **2012**, *48*, 10960–10962; b) A. Monney, F. Nastri, M. Albrecht, *Dalton Trans.* **2013**, *42*, 5655–5660.
[23] R. M. Drost, D. L. J. Broere, J. Hoogenboom, S. N. de Baan, M. Lutz, B. de Bruin, C. J. Elsevier, *European J. of Inorg. Chem.* **2015**, *2015*, 982–996.
[24] A. Monney, E. Alberico, Y. Ortin, H. Müller-Bunz, S. Gladiali, M. Albrecht, *Dalton Trans.* **2012**, *41*, 8813–8821.
[25] a) S. Spreckelmeyer, C. Orvig, A. Casini, *Molecules* **2014**, *19*, 15584–15610; b) M. J. McKeage, S. J. Berners-Price, P. Galettis, R. J. Bowen, W. Brouwer, L. Ding, L. Zhuang, B. C. Baguley, *Cancer Chemother. Pharmacol.* **2000**, *46*, 343–350; c) P. J. Barnard, M. V. Baker, S. J. Berners-Price, D. A. Day, *J. Inorg. Biochem.* **2004**, *98*, 1642–1647.
[26] F. Cisnetti, C. Gibard, A. Gautier, *J. Organomet. Chem.* **2015**, *782*, 22–30.
[27] J. C. Y. Lin, R. T. W. Huang, C. S. Lee, A. Bhattacharyya, W. S. Hwang, I. J. B. Lin, *Chem. Rev.* **2009**, *109*, 3561–3598.
[28] R. J. Ouellette, J. D. Rawn, in *Principles of Organic Chemistry* (Eds.: R. J. Ouellette, J. D. Rawn), Elsevier, Boston, **2015**, pp. 287–314.
[29] a) R. J. Ouellette, J. D. Rawn, in *Principles of Organic Chemistry* (Eds.: R. J. Ouellette, J. D. Rawn), Elsevier, Boston, **2015**, pp. 315–342; b) A. Radzicka, R. Wolfenden, *J. Am. Chem. Soc.* **1996**, *118*, 6105–6109.
[30] a) T. Zou, C. T. Lum, C.-N. Lok, W.-P. To, K.-H. Low, C.-M. Che, *Angew. Chem. Int. Ed.* **2014**, *53*, 5810–5814; *Angew. Chem.* **2014**, *126*, 5920–5924; b) I. Ott, *Coord. Chem. Rev.* **2009**, *253*, 1670–1681; c) I. Tolbatov, C. Coletti, A. Marrone, N. Re, *Inorg. Chem.* **2020**, *59*, 3312–3320.
[31] H. J. Forman, H. Zhang, A. Rinna, *Mol. Aspects Med.* **2009**, *30*, 1–12.
[32] a) N. Estrada-Ortiz, F. Guarra, I. A. M. de Graaf, L. Marchetti, M. H. de Jager, G. M. M. Groothuis, C. Gabbiani, A. Casini, *ChemMedChem* **2017**, *12*, 1429–1435; b) E. B. Bauer, M. A. Bernd, M. Schütz, J. Oberkofler, A. Pöthig, R. M. Reich, F. E. Kühn, *Dalton Trans.* **2019**, *48*, 16615–16625.
[33] a) C. Schmidt, L. Albrecht, S. Balasupramaniam, R. Misgeld, B. Karge, M. Brönstrup, A. Prokop, K. Baumann, S. Reichl, I. Ott, *Metallomics* **2019**, *11*, 533–545; b) C. Schmidt, B. Karge, R. Misgeld, A. Prokop, M. Brönstrup, I. Ott, *MedChemComm* **2017**, *8*, 1681–1689; c) F. Hackenberg, M. Tacke, *Dalton Trans.* **2014**, *43*, 8144–8153.
[34] W. Maenhaut, K. Malmqvist, in *Handbook of X-ray Spectrometry 2nd ed.* (Eds.: R. E. Van Grieken, A. A. Markowicz), Marcel Dekker, Inc., **2002**, pp. 730–821.
[35] L. Côrte-Real, A. P. Matos, I. Alho, T. S. Morais, A. I. Tomaz, M. H. Garcia, I. Santos, M. P. Bicho, F. Marques, *Microsc. Microanal.* **2013**, *19*, 1122–1130.
[36] V. T. Maulik, S. L. Jennifer, J. S. Teruna, *Curr. Protein Pept. Sci.* **2009**, *10*, 614–625.
[37] J. L. Wedding, H. H. Harris, C. A. Bader, S. E. Plush, R. Mak, M. Massi, D. A. Brooks, B. Lai, S. Vogt, M. V. Werrett, P. V. Simpson, B. W. Skelton, S. Stagni, *Metallomics* **2017**, *9*, 382–390.
[38] a) F. Ardito, M. Giuliani, D. Perrone, G. Troiano, L. Lo Muzio, *Int. J. Mol. Med.* **2017**, *40*, 271–280; b) N. Ribeiro, S. Roy, N. Butenko, I. Cavaco, T. Pinheiro, I. Alho, F. Marques, F. Avecilla, J. Costa Pessoa, I. Correia, *J. Inorg. Biochem.* **2017**, *174*, 63–75.
[39] R. Uson, A. Laguna, M. Laguna, D. A. Briggs, H. H. Murray, J. P. Fackler, in *Inorganic Syntheses*, John Wiley & Sons, Inc., **2007**, pp. 85–91.
[40] J. Charton, M. Gauriot, J. Totobenazara, N. Hennuyer, J. Dumont, D. Bosc, X. Marechal, J. Elbakali, A. Herledan, X. Wen, C. Ronco, H. Gras-Masse, A. Heninot, V. Pottiez, V. Landry, B. Staels, W. G. Liang, F. Leroux, W.-J. Tang, B. Deprez, R. Deprez-Poulain, *Eur. J. Med. Chem.* **2015**, *90*, 547–567.
[41] a) A. Veríssimo, L. C. Alves, P. Filipe, J. N. Silva, R. Silva, M. D. Ynsa, E. Gontier, P. Moretto, J. Pallon, T. Pinheiro, *Microscopy* **2007**, 70, 302–309; b) C. C. Marques, A. C. Nunes, T. Pinheiro, P. A. Lopes, M. C. Santos, A. M. Viegas-Crespo, M. G. Ramalhinho, M. L. Mathias, *Biol. Trace Elem. Res.* **2006**, *109*, 075–090.
[42] D. Fontinha, S. A. Sousa, T. S. Morais, M. Prudêncio, J. H. Leitão, Y. Le Gal, D. Lorcy, R. A .L. Silva, M. F. G. Velho, D. Belo, M. Almeida, J. F. Guerreiro, T. Pinheiro, F. Marques, *Metallomics*, **2020** [published online ahead of print].
[43] http://www.microbeams.co.uk/ (accessed June 2020).

Manuscript received: May 21, 2020
Revised manuscript received: June 20, 2020
Accepted manuscript online: June 27, 2020
Version of record online: July 31, 2020